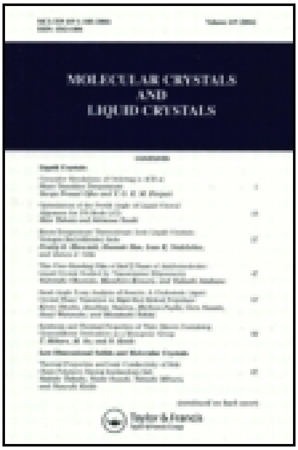

Molecular Crystals and Liquid Crystals Science and Technology. Section A. Molecular Crystals and Liquid Crystals

Vibrational Spectroscopy of Lithium Manganese Spinel Oxides

C. Julien [a], A. Rougier [b], E. Haro-poniatowski [a] & G. A. Nazri [b]

[a] Laboratoire des Milieux Désordonnés et Hétérogènes, Université Pierre et Marie Curie, 4 place Jussieu, 75252, Paris, France

[b] Physics and Physical Chemistry Department, General Motors R&D Center, Warren, MI, 48090, USA

Version of record first published: 04 Oct 2006

To cite this article: C. Julien, A. Rougier, E. Haro-poniatowski & G. A. Nazri (1998): Vibrational Spectroscopy of Lithium Manganese Spinel Oxides, Molecular Crystals and Liquid Crystals Science and Technology. Section A. Molecular Crystals and Liquid Crystals, 311:1, 81-87

To link to this article: http://dx.doi.org/10.1080/10587259808042370

Mol. Cryst. Liq. Cryst., 1998, Vol. 311, pp. 81–87
Reprints available directly from the publisher
Photocopying permitted by license only

Vibrational Spectroscopy of Lithium Manganese Spinel Oxides

C. JULIEN[a], A. ROUGIER[b], E. HARO-PONIATOWSKI[a], and G.A. NAZRI[b]
[a]Laboratoire des Milieux Désordonnés et Hétérogènes, Université Pierre et Marie Curie, 4 place Jussieu, 75252 Paris, France; [b]Physics and Physical Chemistry Department, General Motors R&D Center, Warren, MI 48090, USA

Lithiated spinel manganese oxides with various amounts of lithium have been prepared through solid-state reaction and electrochemical intercalation and deintercalation. Structures of the $Li_xMn_2O_4$ samples with $0.3 \leq x \leq 1.2$ are studied using X-ray diffraction and Rietveld refinement techniques. We report vibrational spectra of lithiated manganese oxides as a function of lithium concentration. The spectra of lithiated spinel manganese oxides have been analyzed on the basis of LiO_4 tetrahedra and MnO_6 octahedra when $Li/Mn \leq 0.5$, and LiO_4, LiO_6, and MnO_6 structural units when $Li/Mn > 0.5$. Electrochemical performances of lithium manganese oxide are also studied.

Keywords: lithium manganese oxide; vibrational spectroscopy; lithium batteries

INTRODUCTION

Spinel lithium manganese oxides as 4-volt cathodes in high energy density lithium batteries are potentially attractive because of their low cost and low toxicity [1-3]. The structural and electrochemical properties of spinel-related MnO_2, usually described by $Li_xMn_2O_4$ have been widely investigated [4-6]. $Li_xMn_2O_4$ has a cubic structure and undergoes weak structural modifications upon delithiation in the compositional range from x=1.0 to x=0.3.

This work reports on the vibrational spectra, i.e., Raman scattering (RS) and Fourier transform infrared (FTIR) absorption of the lithiated spinel manganese oxides. These techniques are capable of probing directly the near-neighbor environment of oxygen coordination around the lithium and manganese cations. Thus, we can consider the spinel $LiMn_2O_4$ vibrational spectra such as the superposition of the spectra of local structures. We study the

FTIR and RS spectra of the spinel $LiMn_2O_4$, its delithiated forms $Li_xMn_2O_4$ with $0.3 \leq x \leq 1.0$, and the lithium intercalated phase $Li_xMn_2O_4$ with $x=1.2$. The normal modes of the spinel $LiMn_2O_4$ are discussed in the O_h^7 spectroscopic symmetry and the vibrations due to lithium ions with their oxygen neighbors are identified.

EXPERIMENTAL

The $LiMn_2O_4$ cathode material was prepared by mixing fine powder of LiOH and MnO_2 in 1:2 mole ratio with 7 mole% excess of LiOH to compensate for the loss of lithium during heat treatment. The mixture was ground inside a dry box filled with argon to prevent carbonate formation. The mixture then was packed in a ceramic boat and heat treated at 470°C for four hours. At this temperature LiOH melts and uniformly coats the MnO_2 grains. The product was then ground to fine powder and heat treated at 750°C for 12 hours under flow of oxygen. The final product was cooled to room temperature under continuous flow of oxygen. Loss of lithium due to evaporation at 750°C has been estimated by elemental analysis to about 7 mole%. The final product of the synthesis was kept inside the dry box for characterization. The delithiated and lithiated $Li_xMn_2O_4$ ($0.3 \leq x \leq 1.2$) samples have been prepared by electrochemical method using a galvanic cell $Li/Li^+/Li_xMn_2O_4$ with a non-aqueous 1M $LiPF_6$ in ethylene carbonate-dimethyl carbonate (65/35 mole ratio) electrolyte. The cathodes were carefully disassembled and rinced with salt free solvent for spectroscopic measurements.

Raman spectra of $Li_xMn_2O_4$ samples were recorded on a Jobin-Yvon U1000 double monochromator using the 514.5 nm radiation from a Spectra-Physics 2020 argon-ion laser. Standard photon-counting techniques were used for detection. Infrared absorption spectra were recorded using a Bruker IFS113 vacuum Fourier transform infrared interferometer. In the far-infrared region, this apparatus is equipped with a 3.5 μm-thick beam splitter, a globar source, and a liquid helium cooled bolometer. Powdered samples were dispersed in solid paraffin which does not exhibit any infrared absorption peak in the studied wavenumber range.

RESULTS AND DISCUSSION

The final composition of the $LiMn_2O_4$ sample determined by elemental analysis for Li and Mn using atomic absorption and inductive coupling plasma emission spectroscopy shows that the calculated stoichiometry of our sample was a lithium-rich manganese oxide spinel (Li/Mn=0.51). Figure 1 displays the X-ray diffraction (XRD) pattern of lithium-rich $LiMn_2O_4$ spinel. Structural refinements are made based on Fd3m space group and calculated intensities are generated using the Siemens Rietveld refinement procedure. A good agreement is obtained between observed and calculated values. Considering the position of the peak attributed to the (400) line, we observed an almost linear decrease of the d-spacing upon lithium deintercalation in the spinel host.

The compositional dependences of the Raman and infrared spectra of the $Li_xMn_2O_4$ spinels, recorded at room temperature, are shown in Figs. 2 and 3, respectively. The RS spectra were recorded with a low power laser excitation of 30 mW to prevent any decomposition of the sample. The RS spectrum of $LiMn_2O_4$ is dominated by a strong and broad band at ca. 625 cm^{-1} with a shoulder at 580 cm^{-1}. A band with a medium intensity appears at ca. 480 cm^{-1}. Three bands having a weak intensity are observed at ca. 365, 304 and 154 cm^{-1}. A broad and very weak band is also observed at ca. 198 cm^{-1}. The FTIR spectrum is dominated by two strong absorption bands at ca. 619 and 513 cm^{-1}. Three weak bands are observed in the low frequency region at ca. 225, 277 and 370 cm^{-1}. A weak band is appeared out at ca. 440 cm^{-1}.

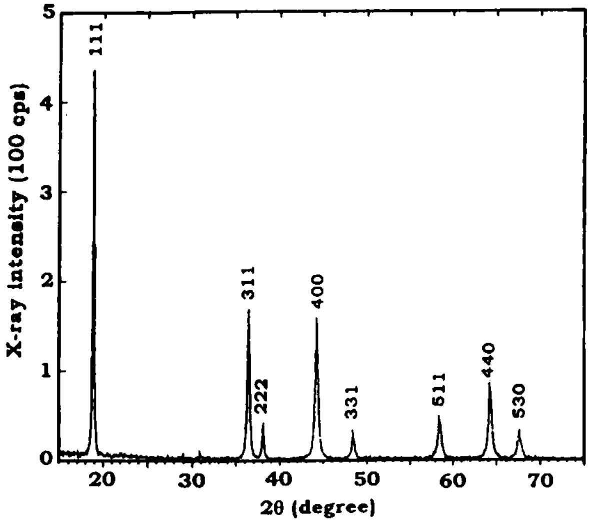

FIGURE 1 X-ray diffraction pattern of lithium-rich $LiMn_2O_4$ spinel.

The cubic spinel possesses Fd3m symmetry and has a general structural formula $Li[Mn_2]O_4$, where the manganese cations reside on the octahedral 16d sites, the oxygen anions on the 32e sites, and the lithium ions occupy the tetrahedral 8a sites. Analysis of the vibrational spectra of $LiMn_2O_4$ with Fd3m space group yields nine optic modes: five modes are Raman active ($A_{1g}+E_g+3F_{2g}$) and four are infrared active (F_{1u}). It is also convenient to analyse these spectra in terms of localized vibrations, considering the spinel structure built of MnO_6 octahedra and LiO_4 tetrahedra [7]. Results are summarized in Table I.

The Raman band located at ca. 625 cm^{-1} can be viewed as the symmetric Mn-O stretching vibration of MnO$_6$ groups. The position and the halfwidth of this band remain almost unchanged upon delithiation. This band is assigned to the A_{1g} symmetry in the O_h^7 spectroscopic space group. Its broadening may be related with the cation-anion bond lengths and polyhedral distortion occurring in LiMn$_2$O$_4$. The intensity of the shoulder located at 580 cm^{-1} increases upon lithium deintercalation. This may be due to the change of Mn^{3+} and Mn^{4+} proportion vs. x in the material. It is a fact that Li[Mn^{3+}Mn^{4+}]O$_4$ is a small-polaron semiconductor [8]. The RS peak at 304 cm^{-1} has the E$_g$ symmetry whereas the peaks located at 154, 365 and 480 cm^{-1} have the F$_{2g}$ symmetry.

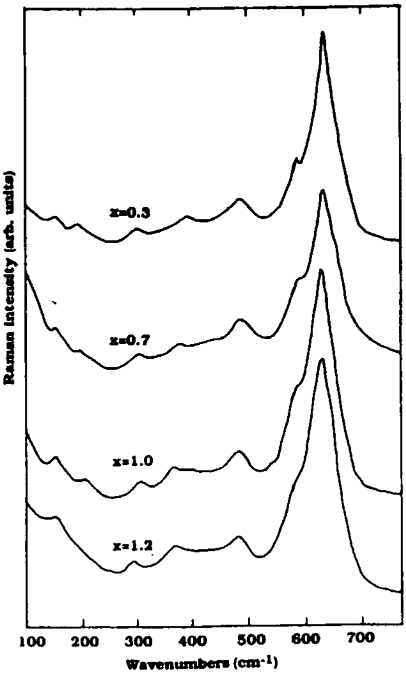

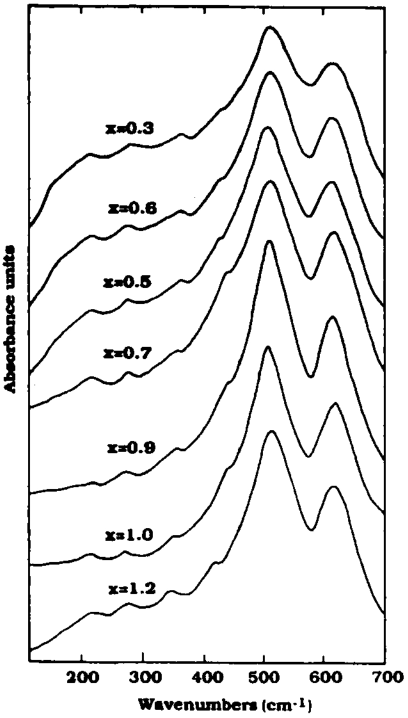

FIGURE 2 Raman scattering spectra of the spinel Li$_x$Mn$_2$O$_4$ as a function of the lithium content with $0.3 \le x \le 1.2$. These spectra were recorded using a 514.5 nm Ar$^+$ laser line at 30 mW power excitation.

FIGURE 3 Far-infrared spectra of the spinel Li$_x$Mn$_2$O$_4$ as a function of the lithium content with $0.3 \le x \le 1.2$.

The high-frequency bands of the FTIR absorption spectrum of $LiMn_2O_4$ located at ca. 619 and 513 cm^{-1} are attributed to the asymmetric stretching modes of MnO_6 group whereas the low-frequency bands at ca. 225, 277 and 370 cm^{-1} are assigned to the bending modes of Mn-O. Because FTIR spectroscopy is capable of probing directly the near neighbor environment of the cation, we can study the local environment of lithium ions in this material. The vibrational frequency of the LiO_4 tetrahedron has appeared out at 435 cm^{-1} in the spinel $LiFeCr_4O_8$ [9]. It has been also demonstrated that the IR resonant frequencies of alkali metal cations in their equilibrium positions in inorganic oxide glasses are as cation mass dependent bands. Thus, the IR resonant frequency is related to the local force constant with an effective mass of vibration which is roughly that of alkali ion [10]. This leads to the frequency at ca. 440 cm^{-1} for oscillation of the Li^+ ion with O^{2-} near neighbors in $LiMn_2O_4$.

TABLE I. Wavenumbers (in cm^{-1}), intensity[a], and assignments of the Raman- and IR-active modes of the spinel $LiMn_2O_4$.

Raman	Intensity	IR	Intensity	Assignment
154	w			δ(Mn-O)
198	w	225	w	
		277	w	
304	w			δ(Mn-O)
365	w	370	w	δ(Li-O)
		440	w	ν(Li-O)
480	m			
		513	S	ν(Mn-O)
580	s			
		619	S	ν(Mn-O)
625	S			

[a] w=weak, m=medium, s=shoulder, S=strong.

The Raman and IR spectra of the delithiated phases of $Li_xMn_2O_4$ have the same shape as the spinel $LiMn_2O_4$. The Raman peaks have almost the same frequency for all the composition range $0.3 \leq x \leq 1.0$. Only the peak located at ca. 365 cm^{-1} shifts significantly upon lithium deintercalation. Thus the resonance frequency at 365 cm^{-1} is an indication that the configuration of the F_{2g} mode is predominantly due to Li-O bonding. The increase in frequency of this mode is in good agreement with the structural modification of the spinel phase upon Li deintercalation. When Li/Mn>0.5, the local environment of oxygen anions around lithium cations changes. The FTIR spectrum displays a peak located at 410 cm^{-1}, which is attributed to the vibrational frequency of LiO_6 octahedra.

These results agree with the lithium occupancy in octahedral 16c sites reported by Ohzuku et al. [2]. Other vibrational modes of the MnO_6 structural units remain unchanged in the lithiated sample. Similar Raman and IR spectra are obtained on lithiated $Li_xMn_2O_4$ (x=1.18) sample prepared by solid-state reaction.

It can be stated that in the ideal cubic spinel $LiMn_2O_4$, the Mn^{3+} and Mn^{4+} cations are considered as crystallographically equivalent (16d sites) in agreement with XRD data; then, occupation probabilities of 0.5 must be affected for each cation in 16d. Hence, a loss of translation invariance certainly occurs, due to local lattice distorsions around the different Mn^{3+} and Mn^{4+} cations. As a result, a breakdown in the Raman and IR selection rules is expected, which may explain the observation of broads bands (disorder) and the fact that more modes than expected are observed in cubic $LiMn_2O_4$. Furthermore, this would be consistent with the fact that the $LiMn_2O_4$ spectra are not markedly different from those of $Li_xMn_2O_4$ where, of course, disorder necessarily takes place because of the non stoichiometry.

The rechargeability of the $Li//LiMn_2O_4$ cell was examined at 0.2 mA/cm^2 current density between 3.5 and 4.5 V. The upper plateau provides over 130 mA h/g with an excellent cyclability. The capacity loss is about 10% of initial capacity and the loss factor is 0.15% per cycle. Considering the low loss factor upon charge-discharge cycling, we can conclude that our sample is able to deliver a rechargeable capacity of more than 100 mA h/g for long cycles.

CONCLUSION

These infrared and Raman studies of lithium manganospinels show that: (a) the deintercalation of Li ions from the host does not affect the structural MnO_6 entities of the framework; the vibrational modes of the MnO_6 groups remain stable in frequency and intensity. (b) some vibrational modes in the intermediate frequency region (300-400 cm^{-1}) have been recorded; these modes are assigned to the vibrations of lithium cations against the neighboring oxygen anions. (c) a small frequency shift is attributed to a weak variation in the bonding and force constants upon lithium deintercalation. A loss of translation invariance certainly occurs; due to local lattice distorsions around the different Mn^{3+} and Mn^{4+} cations. As a result, a breakdown in the Raman and IR selection rules is expected, which may explain the observation of broads bands (disorder) and the fact that more modes than expected are observed in cubic $LiMn_2O_4$. The vibrational features of the Li electrochemically intercalated $Li_{1.2}Mn_2O_4$ show a new band located at 410 cm^{-1}. This band is attributed to the vibrational mode of LiO_6 octahedra.

References

[1.] M.M. Thackeray, P. Johnson, L. de Piciotto, P.G. Bruce, and J.B.

Goodenough, *Mater. Res. Bull.*, **19**, 179 (1984).

[2.] T. Ohzuku, M. Kitagawa, and T. Hirai, *J. Electrochem. Soc.*, **137**, 769 (1990).

[3.] D. Guyomard and J.M. Tarascon, *J. Electrochem. Soc.*, **139**, 937 (1992).

[4.] J. Barker, R. Pynenburg, and R. Koksbang, *J. Power Sources*, **52**, 185 (1994).

[5.] A. Yamada, K. Miura, K. Hinokuma, and M. Tanaka, *J. Electrochem. Soc.*, **142**, 2149 (1995).

[6.] C. Julien, A. Rougier, and G.A. Nazri, *Mater. Res. Soc. Symp. Proc.*, **393** (1997).

[7.] H.D. Lutz, W. Becker, B. Muller, and M. Jung, *J. Raman Spectrosc.*, **20**, 99 (1989).

[8.] J.B. Goodenough, A. Manthiran, and B. Wnetrzewski, *J. Power Sources*, **43-44**, 269 (1993).

[9.] J. Preudhomme and P. Tarte, *Spectrochim. Acta*, **27A**, 845 (1971).

[10.] G.J. Exarhos and W.N. Risen, *Solid State Commun.*, **11**, 755 (1972).